Characterization of Artifactual Correlation in Highly-Accelerated Simultaneous Multi-Slice (SMS) fMRI Acquisitions

Kawin Setsompop[1,2], Jonathan Polimeni[1,2], Himanshu Bhat[3], and Lawrence L Wald[1,2]

[1]*A.A. Martinos Center for Biomedical Imaging, MGH, Charlestown, MA, United States,* [2]*Harvard Medical School, Boston, MA, United States,* [3]*Siemens Medical Solutions, Charlestown, MA, United States*

Target audience: fMRI investigators; neuroimaging scientists and clinicians.

Purpose: Simultaneous Multi-Slice (SMS) acquisition (1-5) with blipped-CAIPI scheme (6) has enabled dramatic reduction in imaging time for EPI-based fMRI acquisitions, enabling high-resolution whole-brain acquisitions with short repetition times. The characterization of SMS acquisition performance is crucial to wide adoption of the technique. The g-factor (7) and leakage-factor (8,9) have been proposed as metrics for assessing the SMS acquisition's noise and signal leakage artifacts, respectively. In this work, we examine another important source of artifact: spurious thermal noise correlation between aliased imaging voxels. This artifactual correlation can create undesirable bias in fMRI resting-state functional connectivity analysis, particularly for low-SNR acquisitions, e.g., acquisitions with high spatial resolution and/or short TR where thermal noise is the dominant noise source. Here we provide a simple method for characterizing this spurious thermal noise correlation, which should aid in guiding the selection of appropriate slice- and inplane-acceleration factors for SMS acquisitions during protocol design.

Methods: The calculation of thermal noise correlation between voxels can be performed using a Monte-Carlo simulation via the pseudo-multiple replica method (7). From the synthetic time series with added noise, a correlation coefficient between any pair of voxels in the final reconstructed image can be calculated to quantify the amount of correlation induced by the undersampling of the data and the specifics of the image reconstruction. Because thermal noise correlation occurs only between voxels lying at locations in the fully-sampled image that are superimposed in the aliased image, here correlation maps will only be presented for these voxel pairs. To assess the performance of various acquisition protocols, multi-slice GRE-EPI data (FOV: 208×208×120 mm^3 , 2 mm isotropic voxel size) were acquired on a Tim Trio 3T scanner (Siemens Healthcare, Erlangen Germany). Monte-Carlo simulations were performed for acquisitions with (i) SMS acceleration factor 5 and (ii) SMS acceleration factor 3 with in-plane acceleration R=2, both at various inter-slice FOV shift factors allowed by the blipped-CAIPI scheme. Slice-GRAPPA and GRAPPA algorithms were used to perform slice and in-plane unaliasing, respectively. G-factor and thermal noise correlation are reported and compared.

Results: Fig. 1 shows thermal noise correlation coefficient maps of voxels in the fourth imaging slice with voxels in the other slices for SMS 5 acquisitions at various FOV shift factors. The correlation coefficients and 1/g-factors (mean +/− std) over the 5 slices, for FOV shift factor 0, 2, 3, 4, are: 0.28+/–0.20, 0.15+/–0.17, 0.09+/–0.07, 0.17+/–0.14, and 0.45+/–0.15, 0.96+/–0.27, 1+/–0.23, 0.9+/–0.17, respectively. In Fig. 1, for the case with no FOV shift, large correlation can be observed—particularly at slices that are spatially near to slice 4 (i.e., slices 3 and 5). Examining the GRAPPA kernels of these slices showed a similarity in (i) the sets of coils with dominant GRAPPA kernel weights, and (ii) the magnitude of these weights, explaining the resulting high correlation. It can be seen in Fig. 1 that the inter-slice noise correlation is substantially reduced by the blipped-CAIPI method. Note that the trend of high correlation values between spatially nearby aliased voxels still persists in the FOV shifted cases. For FOV/2 shift, the correlation coefficient of slice 4 is highest with slice 2, between which there is effectively no relative inter-slice shift. The correlation coefficients are lowest for FOV/3 shift case, where the optimal spatial separation of the aliasing voxels is achieved. The g-factor penalty follows a similar trend as the correlation coefficient, with the highest retained SNR in FOV/3 shift case. It is important to note that the correlation can still remain relatively high even when the g-factor penalty is mild, such as in the case of FOV/2 shift where the retained SNR is 0.96. Fig. 2 shows the results for SMS3 + inplane2 acquisition at various FOV shifts. The correlation coefficient maps are shown for voxels in the bottom half of slice 2 to the five positions where this region is aliased. The correlation coefficient and 1/g-factor for shift factors 0, 2, 3 are: 0.2+/–0.19, 0.13+/–0.11, 0.14+/–0.12 and 0.74+/–0.1, 0.9+/–0.07, 0.85+/–0.07, respectively. Again, large correlations between aliased voxels that are spatially close together can be observed. For this combination of slice and in-plane accelerations, FOV/2 shift provides the best separation of aliased voxel positions and thus the smallest correlation.

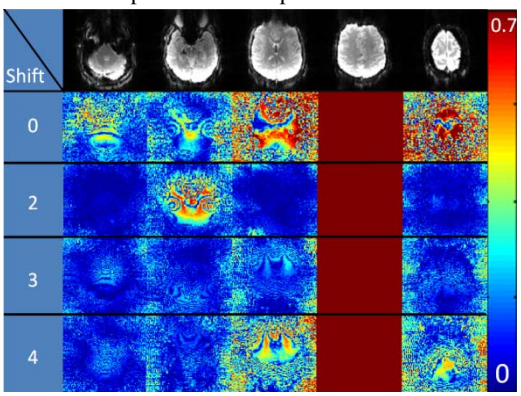

Figure 1: Correlation coefficient maps for SMS 5

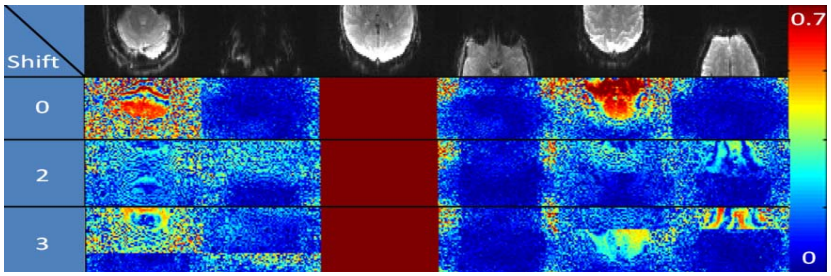

Figure 2: Correlation coefficient maps for SMS3 + inplane2 acquisition

Conclusion: Thermal noise correlation between aliased voxels in highly-accelerated SMS acquisitions can cause undesirable bias in resting-state fMRI correlation analysis. Characterization of this thermal noise correlation was performed using Monte-Carlo simulation, and various blipped-CAIPI schemes were shown to significantly reduce this undesirable correlation. The value of the correlation follows a similar trend to that of the g-factor penalty. However, it is possible for this spurious correlation to be relatively high even while the g-factor penalty is low. Therefore, calculation of this thermal noise correlation should be performed prior to imaging protocol selection, particularly for low-SNR SMS acquisitions.

Support: NIBIB R00EB012107, NIBIB R01EB006847, NCRR P41RR14075 and the NIH U01MH093765 The Human Connectome project. **References: 1.** Larkman DJ. et al, JMRI 2001**2**. Breuer FA. et al, MRM2005 **3.** Nunes RG. et al, ISMRM2006:293 **4.** Moeller S. et al, MRM 2010. **5.** Feinberg DA. et al. PlosOne: 2010 **6.** Setsompop K. et al, MRM 2012 **7.** Robson PM. et al, MRM 2008 **8.** Moeller S. et al, ISMRM 2012:519 **9.** Cauley S. et al, ISMRM 2012:2543